Forecast Accuracy with Optimum Vertical Model Truncation

FERDINAND BAER

Department of Meteorology, University of Maryland, College Park, Maryland

YUEJIAN ZHU

General Sciences Corporation, Laurel, Maryland

(Manuscript received 24 July 1991, in final form 11 March 1992)

ABSTRACT

The National Center for Atmospheric Research Community Climate Model 1 was used as an experimental prediction model to assess the value of reassigning model levels in the vertical based on an optimizing hypothesis. The model was considered for T31 horizontal truncation and 12 vertical levels. The levels were relocated in a model called *test*, and the model with the conventional levels was denoted *standard*. Both models were integrated for 5 days with six independent initial states, and the results were composited. Analyses of the composites for both models were compared to actual observations. The results of the experiments indicate that the barotropic component of the flow was predicted with equal quality by both models but that the baroclinic component was predicted better by the test model. This observation may be explained by the increased fidelity of the vertical structure in the test model, since it has more resolution in the stratosphere.

Additional analyses were performed using a hypothesized three-dimensional scale index that relates the vertical to the horizontal truncation. The results of those analyses were sufficiently suggestive to encourage further studies to find optimum truncation in all three dimensions simultaneously.

1. Introduction

Current numerical weather prediction models produce successful forecasts despite the fact that the discrete representation of prediction equations is not selected by a systematic process designed to optimize forecast results and minimize nonlinear aliasing errors. It is our contention that discovery and utilization of a completely systematic truncation procedure should lead to further improvements in model forecasts, and it is the purpose of this report to provide some information on advances toward the development of an optimum truncation technique.

The process required to convert a nonlinear set of equations to computational form is to create a finite vector set of unknown quantities that represent the dependent variables, and develop a time-extrapolation process whereby that vector set can be calculated into the future from a known initial vector. How this vector is chosen and how it should be truncated is basically the issue that we will consider. Traditionally, the vector is chosen on a grid of points that represents the geometric domain spanned by the variables. Since the domain of the atmosphere is three dimensional, a three-dimensional set of points is selected. Alternately, if the variables can be represented by some global functions, the vector set will be represented by the coefficients of those global functions. This latter procedure is generally known as the "spectral method" and may be applied in any or all of the three dimensions, although little success has yet been achieved by using an expansion in the vertical dimension. The question to be answered is how the grid points are to be chosen (or which global functions are to be used), how the total set is to be truncated (a necessary condition to create a soluble problem), and finally, how the truncation should be coupled in all three dimensions.

Numerical analysis indicates that, because the applicable equations are differential equations in space, equal spacing of points should be most efficient. Moreover, simple scale analysis suggests that scale decomposition of functions represented on a uniform grid will accommodate all scales from the largest possible over the domain to the smallest, which has a length equal to two grid intervals. The global-function approach also allows a scale representation since each global function will describe some scale. In addition, the number of scales thereby represented could also span the same set given by a specified grid of points. The choice of global functions, however, is somewhat discretionary, although some sets are clearly preferable to others, depending on the relevant dynamics and domain of interest.

Corresponding author address: Dr. Ferdinand Baer, Department of Meteorology, 2213 Computer and Space Science Building, University of Maryland, College Park, MD 20742.

© 1992 American Meteorological Society

Some insight into the nature of global functions that might be suitable to the atmospheric prediction problem may be gained by performing an empirical orthogonal function (EOF) analysis of the dependent variable fields to be represented. This has been done several times (see, for example, Holmström 1964; Baer 1974; Bradley and Wiin-Nielsen 1968) for the flow field and the temperature field. Such functions could be used as the global basis functions in a prediction model. Unfortunately, although these functions describe much of the atmospheric variance in the mean, they are very sensitive to time fluctuations and may not always be suitable; in particular, they are highly sensitive to seasonal changes. Moreover, models using such functions are exceptionally complex to create and program for computation, and may be very inefficient.

Perhaps a more appropriate procedure for developing global functions and corresponding scales is to generate them from the model itself. Although nonlinear systems do not have characteristic solutions from which such functions can be determined, linear systems do have eigensolutions, and we can find reasonable global functions by linearizing the prediction equations. If we linearize on a realistic basic state, the global functions are coupled in all dimensions and are far too complex to prove useful. Consequently, the equations are normally linearized about a state of rest (a highly simplified condition), and the resulting linear equations decouple dimensionally and allow for a set of global functions in each dimension independently. Since scales are associated with each function (they are eigenvalues of the eigenfunctions), truncation can be made scale dependent and realistic truncation can be assessed by noting the amount of variance associated with each function when observed data is projected onto it. This procedure does not determine, however, the appropriate truncation of the entire three-dimensional system in terms of truncation in each of the separate dimensional global-function sets.

Applying the simplified linearization (alluded to above) to the atmospheric prediction system—motion equations, continuity, and thermodynamic equations—separation leads to the shallow-water equations for the horizontal dependence and a vertical-structure equation depending on some static-stability distribution. The separation constants are associated with the various equivalent depths of the finite atmosphere. The shallow-water equations are solved in terms of two independent global-function sets, Fourier series in longitude, and Hough functions in latitude. Since Hough functions can be expressed as series of associated Legendre polynomials (and these polynomials are more simple to manipulate), the global functions in latitude are generally represented by them. Scales in terms of wavelengths are easily defined from these two global function sets. Moreover, it is shown that if scaling is associated with the Laplace operator, only the scales related to the Legendre polynomials need be considered in the horizontal domain. Projection of atmospheric data on selected horizontal surfaces in terms of these functions indicates that maximum amplitude resides in the largest scales and decays rapidly with decreasing scale. Thus, scale truncation in the horizontal achieved by cutting the expansion series at some index in the shorter scales is meaningful and is, of course, done regularly.

If spectral functions based on the linearized vertical-structure equation were usable in a model, vertical scaling could be associated with the separation constants (denoted as equivalent depths), and thus, a set of vertical-scaling indices would be available to determine three-dimensional scaling. Unfortunately, it proves more practical to use a gridpoint representation in the vertical, thereby requiring a finite-difference approach to the vertical-structure equations as well as a coupled finite-difference, spectral representation for the fully three-dimensional model. Since the equivalent depths for the vertical-structure problem differ depending on whether one solves the differential equation or a difference equation on a set of grid points, appropriate scaling in the vertical is not clearly evident. Several studies in the last few years suggest that scales associated with the equivalent depths determined from the differential equation solutions to the vertical-structure problem are appropriate (see, for example, Staniforth et al. 1985; Sasaki and Chang 1985). To make the vertical scaling appropriate on a grid of points, Baer and Ji (1989)—to be hereafter denoted as BJ89—developed a procedure that adjusts the points in such a way that the eigenvectors of the differential vertical-structure problem are orthogonal on these adjusted vertical grid points. The difference in vertical scales (equivalent depths) between such a carefully selected grid and a more arbitrarily chosen one can be seen; for example, by comparing the eigenvalues derived by BJ89 to those given by Kasahara and Puri (1981).

If one represents the atmospheric prediction system by an expansion in global functions horizontally and on a selected vertical grid over which the vertical-structure functions are orthogonal, scaling is available in each dimension and potential scale truncation is possible, which might optimize a forecast by minimizing nonlinear aliasing. As a preliminary to studying this problem, BJ89 demonstrated through integrations with the National Center for Atmospheric Research Community Climate Model 0 (NCAR CCM0), using both standard levels and optimally selected levels in the vertical based on their procedure, that forecasts are sensitive to this type of scaling in the vertical. Because of severe model simplifications, however, it was not possible to compare the forecast results to the real atmosphere. Subsequently, Ji and Baer (1992) showed that by application of the quasigeostrophic potential-vorticity equation, as first suggested by Charney (1971),

the scale indices in the horizontal and vertical could be coupled and a three-dimensional scaling index could be derived. Experiments, again with the NCAR CCM0, indicated that errors due to nonlinear dynamics can be minimized by appropriate three-dimensional scale truncation and that such truncation is consistent with the truncation based on the aforementioned three-dimensional index.

Since sensitivity to selecting appropriate vertical scaling has been demonstrated, the next step is to determine whether improved forecasts can be achieved by this procedure. Experiments with the NCAR Community Climate Model 1 (CCM1) have been performed to test for forecast improvements, and it is the results of those experiments that will be reported herein. The NCAR CCM1 was selected as a possible model for such a test, but it does not contain many of the detailed forecast qualities that would make the test highly definitive. In particular, we know that detailed representation of the boundary layer is essential to good forecasting, but the CCM1 does not include much detail in that domain. Thus, we have chosen not to separate out levels in the boundary layer. In a continuing study currently underway with the National Meteorological Center (NMC) global model and recognizing the impact of the boundary layer, we have adjusted the model levels above the boundary layer, keeping the lowest four levels of the model boundary layer unchanged.

Nevertheless, the NCAR CCM1 includes realistic forcing and is a forecast system that has potential for reasonably accurate predictions over a short time scale, up to five days. By comparing forecasts from that model using both optimally selected vertical levels and standard levels with actual observations of the atmospheric system for a number of initial states, we may assess the potential value of using a vertical representation that has more accurate scaling. These experiments, however, were not designed to optimize the truncation three dimensionally, principally because of programmatic difficulties. Plans for such studies are discussed in the Conclusions.

2. Scaling

Our task, to find an optimum three-dimensional model truncation scheme, is twofold. We must establish appropriate truncation in each dimension and find suitable coupling between the linear dimensional representations so that truncation can be established by a single index. A detailed discussion of the problem and its relation to scaling parameters has been presented by Ji and Baer (1992), and we will only summarize here what is needed to describe our study.

Horizontal truncation is customarily determined by truncating a spectral expansion of a global model at some scale index N. Although sophisticated expansion functions, such as Hough functions, are available that accurately describe linearized atmospheric flow (see, for example, Kasahara 1976), accepted present practice is to use associated Legendre polynomials, global functions whose scaling is determined by the order of the polynomial and designated $n \leqslant N$. If the truncation of the expansion set is determined triangularly at the scale index $n = N$, Baer (1972) has shown that n can be considered a two-dimensional scale index in the horizontal domain.

Since models are represented on a numerical grid in the vertical, it is not evident that characteristic structure functions with unique scaling exist that correspond to the aforementioned horizontal scaling. Using linear analysis, characteristic scaling functions that satisfy the vertical-structure equation have been derived (Kasahara and Puri 1981, for example), and their scaling is associated with the equivalent depths that ensue from the solutions. Unfortunately, these structures satisfy the difference equation on the vertical grid and do not necessarily satisfy the differential equation that applies to the problem. BJ89 described a method whereby the vertical grid could be adjusted such that the eigenstructures that satisfy the differential vertical-structure equation are also the eigenstructures on the adjusted grid. The corresponding eigenvalues (equivalent depths) of that solution give scaling to the vertical structures chosen. Thus, an appropriate test of a model's forecast accuracy could be assessed by performing integrations on the appropriately readjusted vertical grid.

The appropriate number of vertical levels and its association with the horizontal truncation based on the index N, however, has not yet been defined. Somehow, the equivalent depths that correspond to vertical-scaling indices should be involved. This question has been addressed by Ji and Baer (1992), and they establish a unique relationship between the horizontal and vertical scaling and, thus, define a three-dimensional scaling index that suggests an optimum truncation for all space dimensions. Their arguments are based on quasigeostrophy of the large-scale atmosphere and follow from the development of the potential vorticity equation, as first considered by Charney (1971) and subsequently by Baer (1981). That equation can be written as

$$\left(\frac{\partial}{\partial t} + \mathbf{V}\cdot\nabla\right)L(\psi) + \frac{\beta}{a\cos\phi}\frac{\partial\psi}{\partial\lambda} = 0, \qquad (1)$$

where notation is standard: $\mathbf{V}$ is the horizontal velocity vector, ψ is the streamfunction, (λ, ϕ) are spherical surface coordinates for longitude and latitude, respectively, and β is the Rossby parameter. Note that L is a three-dimensional space operator,

$$L \equiv \nabla^2 + \frac{f_0^2}{\bar{\rho}}\frac{\partial}{\partial z}\left(\frac{\bar{\rho}}{N^2}\frac{\partial}{\partial z}\right), \qquad (2)$$

involving the vertically dependent density $\bar{\rho}$ and Brunt–Väisälä frequency N; the operator linearly separates the horizontal from vertical dependence. If one chooses the streamfunction to be represented by horizontal eigenfunctions (associated Legendre polynomials) $Y_n^m(\lambda, \phi)$ and vertical eigenstructures, as discussed above and defined as $G_k(z)$, the total streamfunction becomes a series of these eigenfunction products:

$$\psi = \sum_s \psi_s(t) Y_n^m G_k$$

$$s = s(n, m, k). \tag{3}$$

Substitution of (3) into (1) using (2) yields, upon application of the properties of the Legendre polynomials and the structures G_k,

$$s^2(n, k) = n(n+1) + \frac{a^2 f_0^2}{g h_k}, \tag{4}$$

where h_k are the equivalent depths associated with the structures G_k. The indices s have been nondimensionalized, and link the horizontal-scale indices n to the vertical-scale indices h_k.

It might be expected that, for flows that are predominately potential vorticity conserving under the approximations studied, truncation based on a terminating index (s_{max}) might be optimum. This clearly relates the maximum number of vertical levels and corresponding grid points to be chosen (k_{max}) for a selected N truncation index in the horizontal, or vice versa. We will take this scaling procedure into consideration in our subsequent discussions involving model output testing.

How the s index compares to the horizontal index n and the vertical mode, as described by the index k, is shown in Fig. 1. Here we present lines of constant s, chosen by (4) and using equivalent depths selected from Table 2, in the column denoted "test." The significance of this choice will soon become apparent. It is worth noting that if a model is truncated at a fixed vertical mode k and a given horizontal scale n (a choice that is straightforward from a modeling viewpoint), it is *not* truncated for fixed s_{max}. To truncate at s_{max}, spectral-model output must be projected onto the vertical modes and suitably filtered during the integration, unless the model is represented spectrally in all three dimensions, which is a computationally unrealistic expectation at this time.

An analysis of consistent truncation in the spatial domain was presented by Lindzen and Fox-Rabinovitz (1989), and their results support those presented above based on spectral scaling. One limitation to the spectral approach is the requirement that the vertical-structure functions cannot be chosen with geographic dependence. Thus, the tropical modes cannot be different

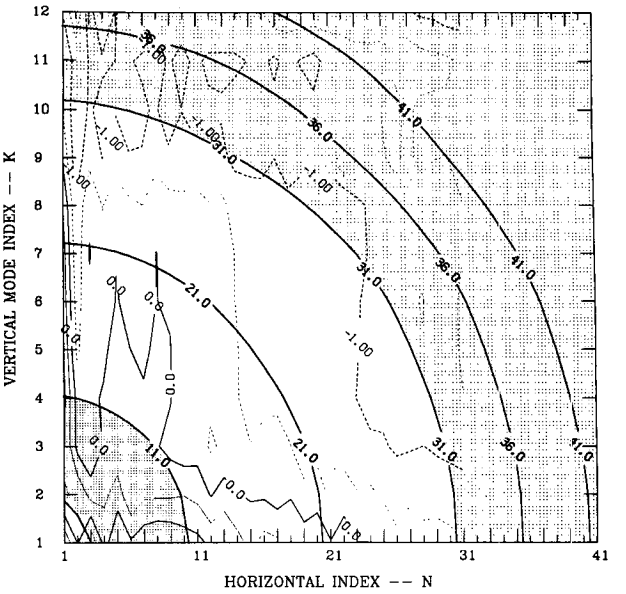

FIG. 1. Isolines of the three-dimensional scale index s as it depends on the horizontal index n and the vertical index k [see Eq. (4)]. Composite s-scale groups s_p, s_l, and s_m are depicted by alternate shading and lack of shading. Analysis of a statistical global data sample of KE as a function of s is superimposed; values are denoted as the logarithms of square meters per second.

from those in the midlatitudes. If the projection of tropical fields onto the selected modes gives a poor representation, then nonlinear aliasing could become a problem. Most models use sufficient resolution so that the structural representation by the modes includes most of the variance in the data. Nevertheless, optimization requires a globally integrated process and cannot be assessed locally. Similar considerations must be given to forcing functions that are projected onto the selected global modes. If the projections are inadequate over much of the domain, serious aliasing problems will arise. Alternately, the integrated effect over the entire domain may prove satisfactory. These effects must be established by model experiments of the type to be presented herein.

3. The model

Ideally, the test for optimum truncation should be made with a perfect model whose only source of error would be truncation. Unfortunately, no such model is available, nor is it practical to experiment with models that demand exceptionally complex reprogramming. We have already tested a piece of the puzzle, the readjustment of levels (see BJ89) with the NCAR CCM0, and found the forecasts to be sensitive to such adjustments. The next step in testing would be to choose a model that has potential for realistic predictions and

to compare predictions from such a model with observations. We have chosen a suitable model and prepared integrations with and without adjusted vertical levels to assess the forecast potential consequent on more appropriate vertical scaling, deferring the test for full three-dimensional truncation to a subsequent study.

The basic model that was chosen was the NCAR CCM1, which has been described in complete detail by Williamson et al. (1987). The model has a significant variety of physics that includes vorticity, divergence, temperature, specific humidity, surface pressure, and soil moisture as dependent variables. Specific physics include radiation, a cloud routine, ozone, convective adjustment, vertical and horizontal diffusion, surface fluxes, and surface energy balance. These features allow the model to provide predictions that might be realistic over a short period of time. Note that it is somewhat deficient in boundary-layer detail.

The model is presented in spectral form on spherical surfaces and uses a finite-difference grid in the vertical (see Bourke 1974). It has various truncation capabilities, and triangular truncation has been selected. Since much of the physics is sensitive to the number of vertical levels and since the number of levels the model was tuned to was 12, 12 levels were chosen for the experiments. Correspondingly, T31 was chosen as the truncation cutoff. If we were to attempt an accurate truncation in a three-dimensional index, as suggested by (4), a 12-level model should be truncated at T36 (see Ji and Baer 1992); however, it proved more convenient programmatically for the experiment to use the T31 truncation.

The model is programmed at a set of vertical levels that are designated as standard. The levels are listed in Table 1, and the top of the model is set at $\sigma = 0$, where σ is the surface pressure normalized vertical pressure coordinate. As noted already, the linearized vertical-

TABLE 1. Vertical sigma levels for the standard CCM1 and our test model. Also listed are the levels at which initial data were available.

Data (hPa)	Test	Standard
10	0.012	0.009
20	0.018	0.025
30	0.026	0.060
50	0.039	0.110
70	0.057	0.165
100	0.084	0.245
150	0.123	0.355
200	0.181	0.500
250	0.265	0.664
300	0.491	0.811
400	0.818	0.926
500	0.984	0.991
700		
850		
1000		

TABLE 2. Equivalent depths associated with the CCM1 for standard levels and for test levels. Note that test-level eigenvalues represent the exact solutions to the vertical-structure equation.

Vertical modes	Standard	Test
1	9689.09	9340.00
2	3169.95	2247.00
3	806.46	702.50
4	281.08	310.50
5	131.86	183.40
6	70.02	125.60
7	30.51	88.06
8	14.24	62.97
9	6.98	47.84
10	2.70	38.76
11	1.06	31.85
12	0.33	26.09

structure equation when solved on the standard grid yields eigenvectors and corresponding eigenvalues that are the equivalent depths. These depths are listed in Table 2. To assess the effect on the model of choosing the standard levels rather than what we consider optimum levels based on scaling considerations, we have calculated the optimum levels for a 12-level model that we denote as test levels, using the optimization technique recommended in BJ89, and these levels are listed in Table 1. For these levels the model top was chosen at $\sigma = 0.01$; this level was selected so that the first interior level at the top would be near the corresponding level in the standard-level set. Moreover, a top level must be selected so that a discrete set of vectors can be established to correspond to the solutions to the ODE representing the aforementioned vertical-structure equations. BJ89 discussed the sensitivity of the vertical structures to the choice of model top. They found that, for a reference model with a fixed top and number of levels, models with more levels and higher tops showed structures in the domain of the reference model that were quite similar to the reference model structures, with (of course) additional structure above the reference top. This suggests, from forecasts in the range of numerical weather prediction as contrasted to climate prediction, that our choice of model top for the test model should be reasonable for comparison with the standard model.

Table 1 demonstrates that the test levels (our current effort at optimum levels) show more resolution in the stratosphere and less in the troposphere; a result that is consistent with the expected variability of vertical structures in the atmosphere in response to the mean thermal stratification. Experiments using a higher resolution in the stratosphere by Boville and Cheng (1988) and Boville and Baumhefner (1990) demonstrate the sensitivity of model predictions to increased stratospheric resolution and the need for such increase to improve forecasting. Moreover, the distribution sug-

gested by BJ89 and used in the test model also substantiates the results of Lindzen and Fox-Rabinovitz (1989). Indeed, this distribution is not far from a logarithmic one, and one could use such a distribution. We determined, however, that the structures that are closest to those for the exact solutions of the ODE arise if one chooses the levels based on the selection process outlined by BJ89. Since we are limited in computing resources, we chose to perform the experiment to be described with those levels that best satisfy the linear system.

The equivalent depths associated with the optimum (test) levels are by definition the eigenvalues of the solutions to the exact differential equation that describes the vertical structure of the linearized prediction equations. Since we choose the first 12 of these solutions (structures), their equivalent depths are listed in Table 2. It is clear that the equivalent depths associated with the standard and test levels differ substantially following the fifth mode. The eigenvectors (structures) associated with these modes also show substantial differences, and details of those differences can be found in BJ89. Because of the nonlinear character of the prediction system, one may anticipate redistribution of energy in the test-level model to be different from that in the model with standard levels. It is these differences and how they relate to the observed evolution of the atmosphere that we will discuss in the following sections.

It should be noted that the model is designed to allow level reassignments. Thus, the forcing functions can be set to accommodate our test levels. However, forcing functions such as those represented by a radiation package are tuned to produce their most realistic results at the standard levels and would require excessive reprogramming to retune them at the test levels. We have not done this.

4. Experiments

The NCAR CCM1 model was used for experimental purposes with the aforementioned 12 levels and T31 truncation. Two companion models were developed for comparison; each integrated with the same initial conditions. The standard model used the vertical levels normally assigned to a 12-level CCM1 configuration, and the test model had modified levels. The levels used can be found in Table 1. Ozone, albedo specifications, and lower-boundary conditions were the same for both models. Radiation calculations were performed every 12 h during the integrations, which used a 15-min time step. Model output was available every 6 h during an integration.

Six integrations were performed with each model, and the results were composited. In this way, the effects on integration of special events in any initial state were minimized, but a realistic number of integrations were chosen to make the computer requirements realistic. Data was selected from the FGGE III SOP1 because it was convenient and because the time sequence of the data allowed for easy comparison of forecasts with observations. To reduce time correlations in the initial states chosen, data were selected at 9-day intervals. The actual datasets used were at 0000 UTC on the following dates: 1 January, 9 January, 17 January, 25 January, 2 February, and 10 February 1979. The data were available on 15 pressure surfaces (see Table 1) and were evaluated at the required model levels by cubic-spline interpolation.

At each output time, data were available in all the dependent variables: vorticity, divergence, temperature, moisture, and surface pressure, including the relevant energies. From each dataset, composites were formed that included global values, values on different vertical surfaces, interpolation to standard levels, and (of course) values assigned to each horizontal and vertical scale, as discussed earlier. We will refer to results in each of these formats subsequently.

5. Results of integrations

To assess the quality of the predictions, we normalize all predicted variables by their initial values and compare the evolution for both the test model (described in the figures as TEST) and the standard model (STD) to the observations (OBS). The maximum time of integration for any experiment was 5 days. We consider first the global properties of the variables. Then, because the principal change in modeling is in the vertical representation, we explore the evolution in terms of vertical scales. Finally, since our ultimate goal is to isolate an optimum three-dimensional scale, we analyze the predictions in terms of the scale index defined by (4).

The variables have all been projected onto the relevant scale components, which include the planetary wavenumber m, the ordinal or two-dimensional index n, and the vertical-mode index k. Note the relationship between m and n for the triangular truncation that has been applied. The amplitudes of various parameters in each scale element (m, n, k) are defined as follows:

$$\text{total KE} \equiv \text{KE}_t = \text{KE}_r + \text{KE}_d;$$

$$\text{rotational KE} \equiv \text{KE}_r = \frac{n(n+1)}{a^2} |\psi_{m,n,k}|^2;$$

$$\text{divergent KE} \equiv \text{KE}_d = \frac{n(n+1)}{a^2} |\chi_{m,n,k}|^2;$$

$$\text{enstrophy} \equiv \text{ES} = \frac{[n(n+1)]^2}{a^4} |\psi_{m,n,k}|^2;$$

and

$$\text{available PE} \equiv \text{APE} = A|T'_{m,n,k}|^2. \quad (5)$$

In (5), ψ represents the streamfunction, χ is the velocity

potential, a is the mean radius of the earth, A is the scaling constant first introduced by Lorenz (1955), and T' is the temperature deviation from its global mean. For composite values, these quantities are averaged over all six integrations, and it is the composites that we shall discuss. To establish global values, the variables are summed over all allowed values of the indices. For values in a vertical mode, the quantities are summed over all allowed horizontal indices. For values in a given three-dimensional scale, quantities are summed over the included n, m, and k indices, as prescribed by (4), noting that contributions from all m indices for a given n must be included.

To determine the forecast quality of any particular wave, such as a baroclinic wave, one must also investigate the evolution of phase. The prediction of individual waves is relevant only when such waves have a significant amplitude. Thus, analysis of phase becomes a complex process, and it is not amenable to conventional statistical analysis of composite values. Since the model we have chosen has serious limitations in its representation of the boundary layer, we felt that detailed analysis of phase was not appropriate. Current experiments in process with the NMC forecast model, however, will be analyzed in detail. Nevertheless, the analysis of amplitudes for the composited data should give a good indication of forecast quality based on level distribution.

The levels of the test model have been chosen to optimize vertical scaling based on the structures of the vertical-structure equation. We have therefore elected to analyze the model output in terms of these structures rather than to perform interpolations to selected pressure levels. Moreover, since the test modes are the best scaling structures available, we have projected all the data (observations, standard model, and test model) onto the test modes. Note that the external mode, because of its reasonable uniformity in height, represents the mean state of the atmosphere quite well, and could therefore be substituted for some mean level like the 500-hPa level. By analogy, the first internal mode should compare well to the large-scale shear field in the atmosphere, say the 700–300-hPa field.

a. *Global characteristics*

We show in Fig. 2 the development in time of the total global kinetic energy as determined from both the test and standard models and as compared to the observations. There is a significant decay in the energy field for both models during the first two days of integration, but the test model recovers much more effectively as prediction time proceeds. That this recovery is a consequence of the superior prediction of the baroclinic rather than the barotropic properties of the test model is supported by Fig. 3b, which shows that the vertical shear of the total vorticity is predicted better by the test model, whereas the mean vorticity as represented by its 500-hPa value is very similar to the standard model output. We use vorticity here because the rotational component of the velocity field is the dominant contributor to the total kinetic energy. Note from Fig. 3a, however, that it is the mean temperature that is predicted better by the test model. This is consistent with the results from the vorticity data insofar as the relationship between the horizontal gradient of mean temperature and vertical shear of rotational flow on the global scale is strong. Whereas it is the mean or barotropic prediction statistics that are traditionally used as a measure of forecast success, the baroclinic component has a dominant impact on the ultimate flow evolution.

b. *Vertical-mode properties*

The principal difference between the test and standard models is the placement of vertical levels and the consequent vertical-structure functions that can be represented. It is thus worthwhile to assess the model predictions in terms of their projections onto the vertical modes. Using all of the observational data available to our experiments, we show statistics of various variables taken from those data and how they distribute in terms of the vertical-structure functions. Figure 4 shows the amplitudes of kinetic energy, enstrophy, and available potential energy [see (5)] projected onto each of the 12 vertical modes denoted by their index k and normalized by their global value. The kinetic energy, enstrophy, and APE are given for projection both onto the test modes and onto the standard modes. It is evident that except for the first three modes there is a significant difference in the amplitude of kinetic energy in the vertical modes of the two models, and substantially more amplitude resides in the higher modes of the test model; a similar observation applies to the en-

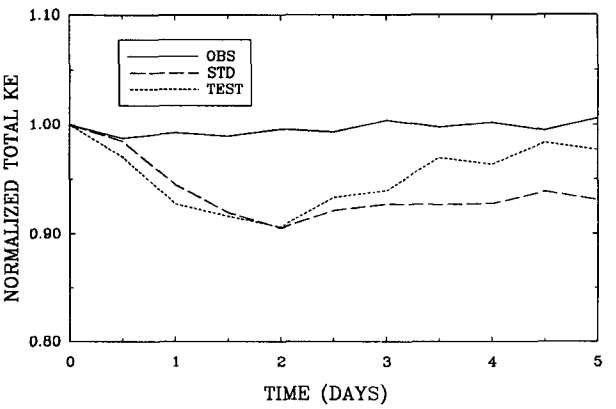

FIG. 2. Global kinetic energy predictions normalized to their initial values for the standard and test models and for the corresponding observations.

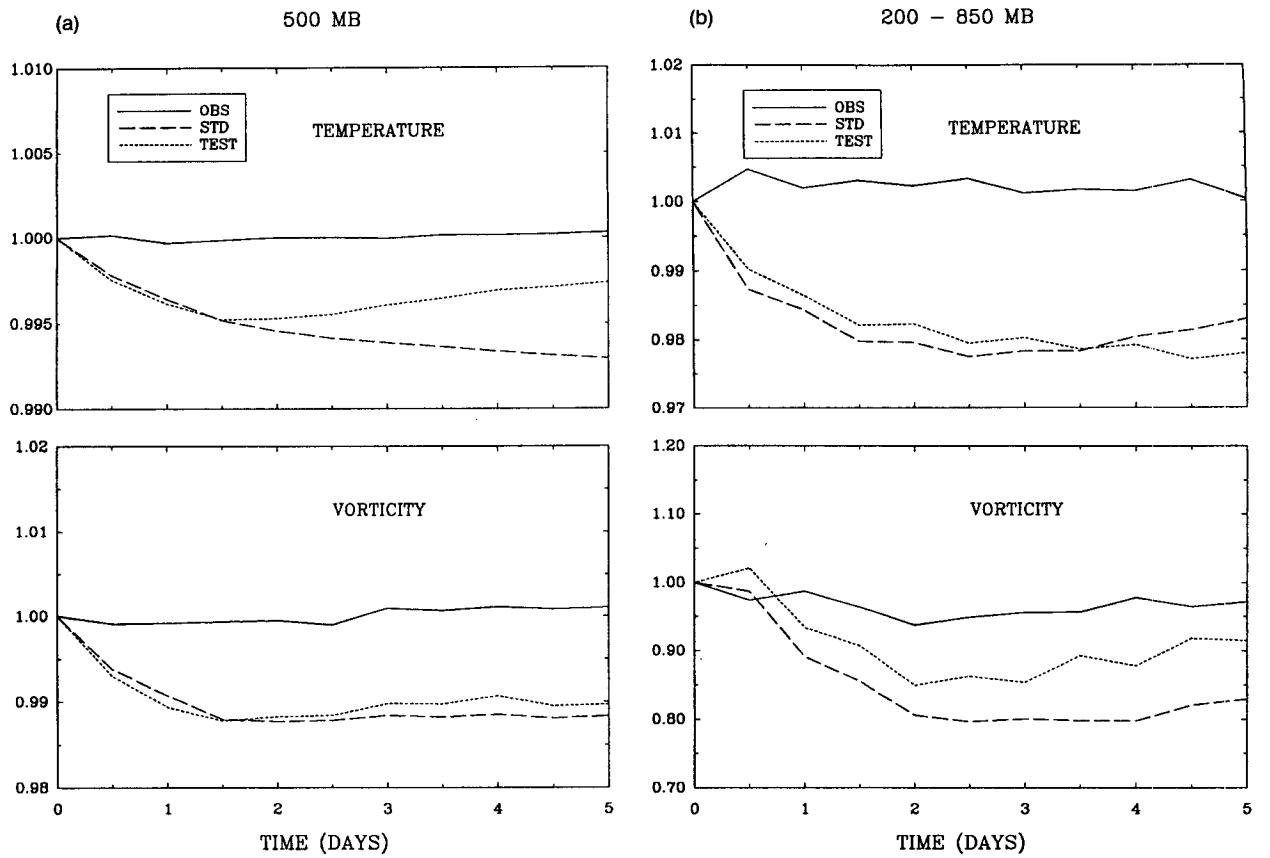

FIG. 3. (a) Global predictions of temperature and vorticity normalized to their initial values on the 500-hPa surface and the corresponding observations. (b) Same as (a) except that values are given for the differences between the 200- and 850-hPa surfaces.

strophy and APE. This is to be expected, since there is more structure in the stratosphere of the test modes and they are able to represent the data in this region more accurately. Because of nonlinear exchange among the scale components, this difference could easily affect the prediction of the lowest and principal energy-containing vertical modes. To identify this process we present Fig. 5. This figure describes the total kinetic energy evolution in each of the first four vertical modes for both models and the observed values as the integration proceeds. Note the consistency of these results with those shown in Fig. 3. Since the first mode is essentially the barotropic mode, projection onto it should correspond to the results seen in the mean atmosphere, which is roughly at 500 hPa. Moreover, the second mode is the primary baroclinic mode, as seen from Fig. 4, and its evolution when comparing the test to the standard model follows the evolution of the shear flow as seen in Fig. 3. This result supports our contention that, by resolving the vertical structure of the atmosphere better in the test model, that model should predict the evolution of the baroclinic part of the flow more successfully.

The kinetic energy projections on the remaining vertical modes ($k > 2$) do not show improved predictions with increasing time for the test model when compared to the standard model and observations. Note, for example, the third mode described in Fig. 5, which is also subject to some diurnal forcing by the model. The higher modes, however, do not contain much energy and may be subject to other modeling defects. Nevertheless, their structure plays a significant role in the time evolution of the lower modes, as is demonstrated specifically by the development of the energy in the second (baroclinic) mode and which is particularly well forecasted by the test model.

c. Three-dimensional scale characteristics

Our goal, as previously stated, is to find a multidimensional coupling of scales so that a global model could be truncated in an optimum way. One possible approach is to develop a three-dimensional scale index, and we have discussed such an index in section 2. Since the redistribution of vertical levels represented in our test model allows for unique scale coupling (in a linear

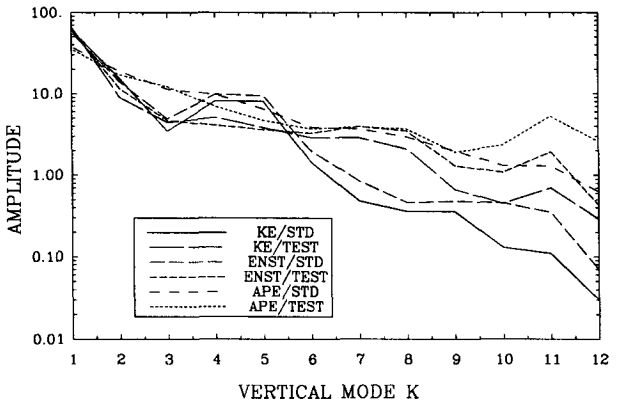

FIG. 4. Distribution of kinetic energy, enstrophy, and available potential energy as a function of vertical modes. Data are composites of all the observational data included in the study and are given as projections onto the standard (STD) and test (TEST) modes.

sense), we present in this subsection the representation of variables projected onto the s index defined by (4). We note that the truncation for our experiments is not optimum with reference to the hypotheses presented by Ji and Baer (1992), nor is the truncation based entirely on a fixed three-dimensional scale index $s = s_{max}$; see for example Fig. 1, which describes s for the truncation at T31 and $k = 12$.

To demonstrate how kinetic energy from the global atmosphere distributes in terms of s scales, Fig. 1 presents the rotational kinetic energy plotted on an n–k diagram, with isolines of s superimposed. Again, note that all values for m scales associated with each n scale must be summed. The data presented are for twice-daily global kinetic energy fields from the FGGE IIIb, SOP1 for 1–6 January 1979. Ideally, if the isolines of kinetic energy were to follow isolines of constant s for suitably large s, truncation at s_{max} would be most appropriate. Although the data show a tendency toward this type of distribution, it would be naive to expect a perfect correlation. The relationship derived for $s(n, k)$ is based on the quasigeostrophic assumption and clearly is inadequate in the tropics. Thus, for this reason alone we cannot expect a perfect correspondence. Nevertheless, since this index is our first approach to three-dimensional scaling, distributions in the s-index domain should prove interesting and insightful.

Our total data sample, whose statistical distribution in vertical modes we described in Fig. 4, can be seen in terms of its distribution with the s index in Fig. 6, where we show the total kinetic energy and enstrophy.

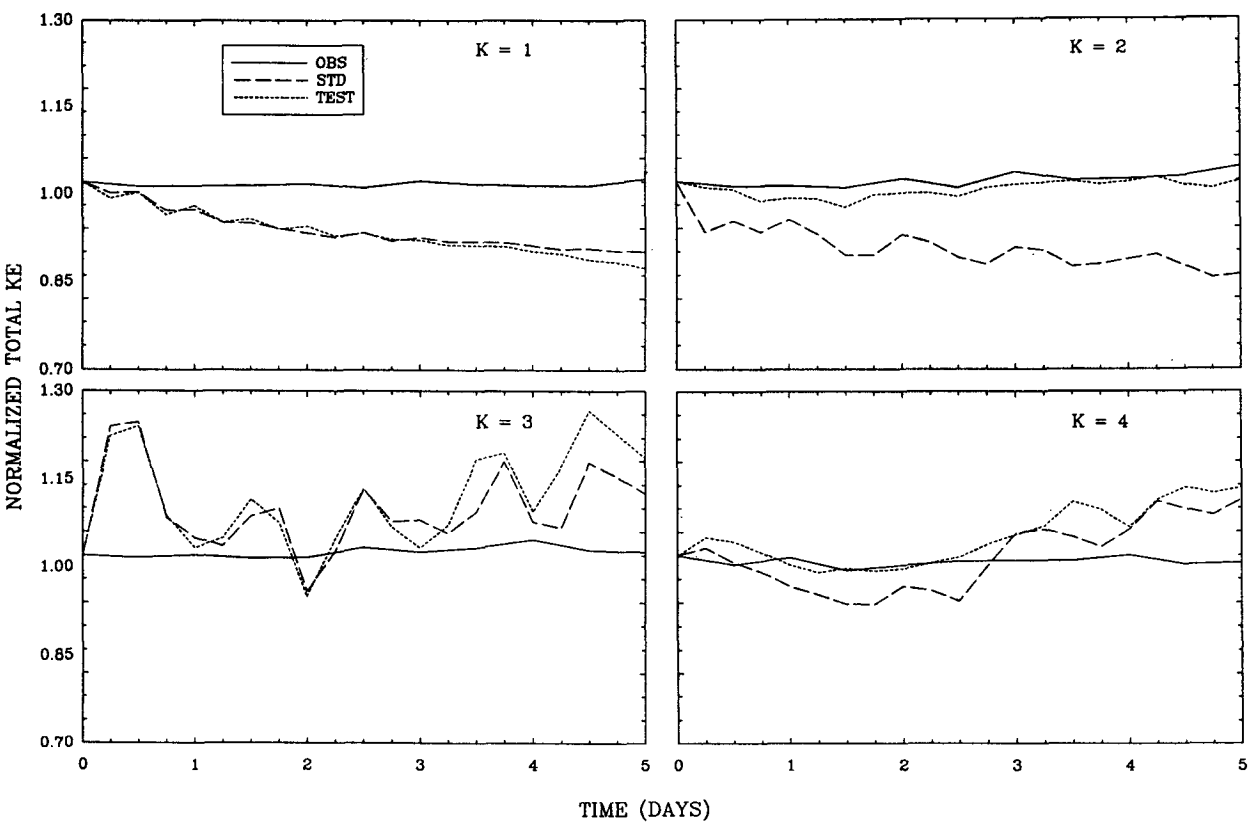

FIG. 5. Total kinetic energy predictions normalized by their initial values and projected onto the first four test vertical modes as produced by the standard and test models and by the corresponding observations.

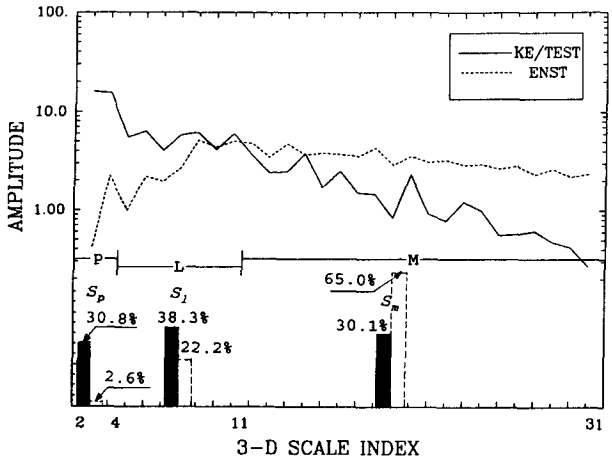

FIG. 6. Kinetic energy and enstrophy of the experimental data projected onto the three-dimensional scale index s using the vertical modes of the test model. The lower bars indicate the composite values for the groups s_p, s_l, and s_m. Solid blocks represent KE, open blocks represent enstrophy.

Note that the logarithmic decay of energy with this scale is approximately -2.25 in the range $11 \leqslant s \leqslant 31$. This is somewhat less steep than the decay with the horizontal scale n for individual vertical-mode projections, which follow more closely the expected statistical -3 decay rate. Additionally, the enstrophy distribution is rather uniform throughout much of the scale range.

For convenience of representation and discussion, we have composited scales into four scale categories as follows:

$$S_p \equiv 1 \leqslant s \leqslant 4; \quad \text{planetary}$$

$$S_l \equiv 4 < s \leqslant 11; \quad \text{long}$$

$$S_m \equiv 11 < s \leqslant 31; \quad \text{medium}$$

$$S_s \equiv 31 < s; \quad \text{short/residual.}$$

Note from Fig. 1, in which these groups are indicated by alternate shading and lack thereof, that S_p (clear) constitutes primarily the largest planetary waves and the external vertical mode; S_l (shaded) includes the lower structured internal vertical modes with the baroclinically active horizontal scales; and S_m (clear) includes the shorter synoptic scales associated with the more highly structured baroclinic vertical modes. The kinetic energy and enstrophy in these groups distribute quite differently from the distributions in other scale composites, as seen from Fig. 6. The kinetic energy in the three principal groups is quite uniform, but the enstrophy increases significantly in the S_m group.

To see how integration variables evolve in this representation, we present Fig. 7. The figure shows the time evolution of enstrophy in the three groups, S_p, S_l, and S_m, and their sum for both the test and standard

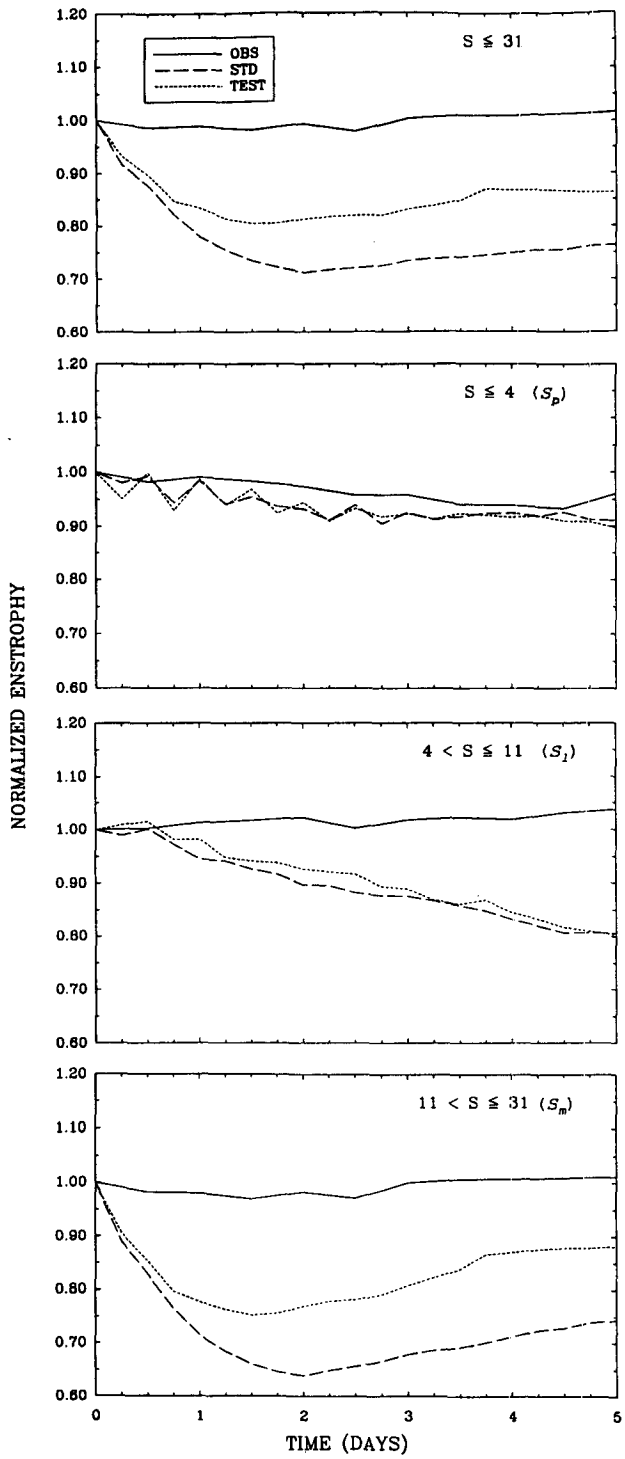

FIG. 7. Predicted enstrophy normalized to its initial value in the composite s groups for the standard and test models and for the corresponding observations. Projections are on the test modes.

models, together with the actual observed data. We see that both the models forecast the S_p group well. This is consistent with our earlier observation that the barotropic component of the flow is well predicted. The larger synoptic scales included in S_l are predicted comparably by both models, but there is significant loss of enstropy relative to observations throughout the integration period. Only in the shorter synoptic scales (S_m) do we note a significant improvement in prediction by the test model when compared to the standard model, which is also reflected in the total composite enstrophy including all scales $s \leq 31$. Despite the somewhat superior prediction by the test model, a significant amount of enstrophy is lost during the prediction that is not reflected by the observations. This may be a consequence of nonsystematic truncation between the vertical and horizontal scales, the failure to truncate at constant s_{max}, or other model deficiences.

6. An optimum truncation experiment

To address the question associated with the effect of truncating a model at a given s_{max}, we performed a preliminary study, integrating the test and standard models for only one set of initial conditions taken from the six initial condition sets defined earlier. It was convenient in terms of model programming to leave the maximum number of vertical levels at 12. The appropriate s_{max} associated with 12 vertical levels, as suggested by the study of Ji and Baer (1992), is 36, which would require a truncation in the horizontal greater than T36 (see Fig. 1 for the abscissa intercept of $s = 36$). We therefore integrated the test and standard models with 12 levels and T42 truncation (a resolution available without significant reprogramming). To assure appropriate truncation to $s_{max} = 36$, the test model output was filtered after each eight integration steps (2 h), and the integration proceeded for 5 days. As noted from Fig. 1, all components (n, k) for which $s > 36$ were filtered.

The integration results may be seen in Fig. 8, where we present the evolution in time of the rotational kinetic energy for both models and observations in the scale group S_l, S_m and for all $s \leq 31$, and the additional filtered test model results that are denoted by the symbol TSTF. It is evident from the composite results for $s \leq 31$ that filtering reduces the energy systematically, whereas the nonfiltered models predict close to the observations. Most of the loss comes in the largest scales, $s \leq 11$, and the filtered model energy stays closer to the observed values during the entire integration period for the S_m group. This reflects a somewhat improved prediction of the energy in the first two internal vertical modes, as may be seen more directly from Fig. 9. It is evident that higher resolution is needed to make this experiment more definitive, since less energy will be lost by filtering a model with higher resolution.

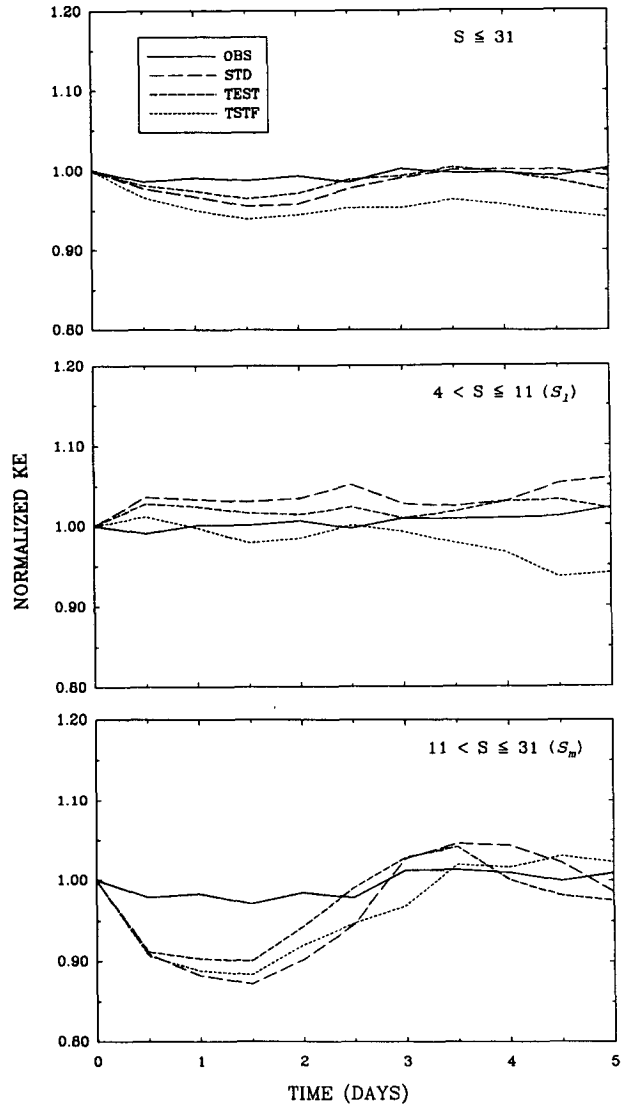

FIG. 8. Same as Fig. 7 but for normalized kinetic energy. Also included is the prediction of the test model that was periodically filtered.

7. Conclusions

Recent studies with alternate placement of model vertical levels suggest that a more systematic approach to assigning those levels in a model and coordinating the choice of both level location and number to the selection of horizontal truncation might yield superior predictions. To test this possibility further, we have performed a series of experiments using the NCAR CCM1 as our base model.

Theoretical considerations provide a formula, discussed in the text, that can be used to optimally place vertical levels. In addition, some indications of the number of levels appropriate to give horizontal trun-

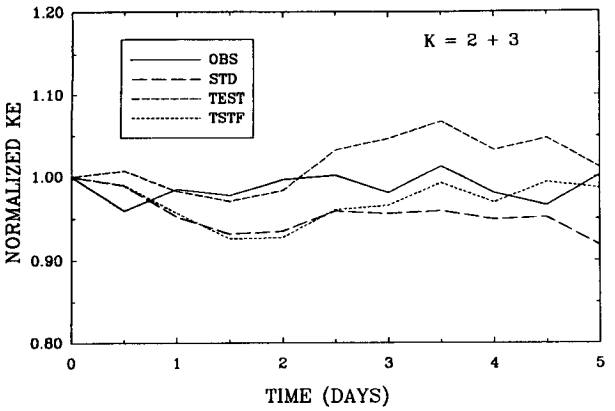

FIG. 9. Predicted normalized kinetic energy projected onto the second and third test vertical modes and summed for the standard and test models, as well as for the filtered test model.

cation are also available. Using this approach, we have integrated the model at T31 for 12 levels, which is also a standard truncation for that model. To average out possible initial-value fluctuations, composites of six independent predictions were used. The model was run at currently used model levels, and it was concurrently run at levels selected to be optimum. The integration results using these two distributions were compared to each other and to observations.

Prediction results show that whereas the barotropic component of the flow was forecast with equal quality by the model with standard levels and the one with the optimum levels, the baroclinic component was forecast more successfully by the optimum-level model. On the global scale this was seen in the mean temperature and in the vorticity shear field. Since the optimum levels distribute with more resolution in the stratosphere, this result suggests that the internal-mode structure of the atmosphere is represented more accurately by the optimally selected levels. An analysis in which the model output was projected onto the vertical modes of the linearized model confirmed the aforementioned result. The energy projected onto the first internal vertical mode was forecast more accurately by the model using the optimally selected levels.

To understand how three-dimensional truncation based on scaling could be used to identify model prediction and perhaps identify skills and deficiencies in models, the forecast output and the corresponding observations were projected onto the three-dimensional scales defined in the text. Interpretation of the forecast data in this mode was somewhat more difficult than in conventional representations, probably because this is a pioneering venture not previously attempted and we have yet no experience explaining data in this format. Nevertheless, the prediction results using more conventional analysis, as noted earlier, could by suitable interpretation be confirmed in this new representation. Finally, an integration in which model data was periodically filtered to simulate optimum three-dimensional truncation showed some promise in successfully predicting the internal structure of the flow variables.

The results described herein are sufficiently encouraging to invite further experimentation. If three-dimensional optimum truncation is to be applied, sufficient resolution is needed so that filtering does not remove significant energy. Moreover, differences in vertical structures between the equatorial and midlatitude regions must be considered and incorporated in any extended composite scale-index hypothesis. While such studies are under way, we have recently performed an integration with the NMC T80, 18-level model, adjusting those levels according to our optimization hypothesis and including boundary-layer levels. Additional integrations are planned with the European Centre for Medium-Range Weather Forecasts (ECMWF) model. These studies should enhance our understanding of the value of model level placement as we proceed with more accurate forecast models.

We have noted that the optimization process places more levels into the stratosphere at the expense of levels in the troposphere. Should more levels be needed in the troposphere to account for physical processes there, the total number of levels must be increased. Such an increase would then require a reconsideration of the horizontal truncation, in particular if optimum three-dimensional truncation is desired, as our experiments suggest. If this problem is thoroughly addressed, a definitive truncation in all dimensions should ensue, which would diminish, if not remove, the need to make arbitrary truncation choices.

Acknowledgments. We appreciate and thank Dr. Ming Ji for his valuable assistance and advice on the project. Additionally, we thank Dr. David Williamson, NCAR, for his assistance and guidance in using the NCAR CCM1. We gratefully acknowledge the NCAR SCD for the computing services necessary to complete our task. This research was supported jointly by the National Science Foundation and the National Oceanic and Atmospheric Administration through Grants ATM-8521374 and ATM-9002835 to the University of Maryland, College Park.

REFERENCES

Baer, F., 1972: An alternate scale representation of atmospheric energy spectra. *J. Atmos. Sci.*, **29**, 649–664.

——, 1974: Hemispheric spectral statistics of available potential energy. *J. Atmos. Sci.*, **31**, 932–941.

——, 1981: Three-dimensional scaling and structure of atmospheric energetics. *J. Atmos. Sci.*, **38**, 52–68.

——, and M. Ji, 1989: Optimal vertical discretization for atmospheric models. *Mon. Wea. Rev.*, **117**, 391–406.

Bourke, W., 1974: A multi-level spectral mode: I. Formulation and hemispheric integrations. *Mon. Wea. Rev.*, **102**, 687–701.

Boville, B. A., and X. Cheng, 1988: Upper boundary effects in a general circulation model. *J. Atmos. Sci.*, **45,** 2591–2606.

——, and D. P. Baumhefner, 1990: Simulated forecast error and climate drift resulting from the omission of the upper stratosphere in numerical models. *Mon. Wea. Rev.*, **118,** 1517–1530.

Bradley, J. H. S., and A. C. Wiin-Nielsen, 1968: On the transient part of the atmospheric planetary waves. *Tellus,* **20,** 533–544.

Charney, J., 1971: Geostrophic turbulence. *J. Atmos. Sci.*, **28,** 1087–1095.

Holmström, I., 1964: On the vertical structure of the atmosphere. *Tellus,* **16,** 288–308.

Ji, M., and F. Baer, 1992: Three-dimensional scaling and consistent truncation of global atmospheric models. *Mon. Wea. Rev.*, **120,** 131–148.

Kasahara, A., 1976: Normal modes of ultra-long waves in the atmosphere. *Mon. Wea. Rev.*, **104,** 669–690.

——, and K. Puri, 1981: Spectral representation of three-dimensional global data by expansion in normal mode functions. *Mon. Wea. Rev.*, **109,** 37–51.

Lindzen, R. S., and M. Fox-Rabinovitz, 1989: Consistent vertical and horizontal resolution. *Mon. Wea. Rev.*, **117,** 2575–2583.

Lorenz, E. N., 1955: Available potential energy in the atmosphere and the maintenance of the general circulation. *Tellus,* **7,** 157–167.

Sasaki, Y. K., and L. P. Chang, 1985: Numerical solution of the vertical structure equation in the normal mode method. *Mon. Wea. Rev.*, **113,** 782–793.

Staniforth, A., M. Béland, and J. Côté, 1985: Numerical solution of the vertical structure equation in sigma coordinates. *Atmos. Ocean,* **23,** 323–358.

Williamson, D. L., J. T. Kiehl, V. Ramanathan, R. E. Dickinson, and J. J. Hack, 1987: Description of NCAR Community Climate Model (CCM1). NCAR Tech. Note, NCAR/TN-285+STR, Boulder, CO, 112 pp.